

Supplementary Information for

Controlling the material properties and rRNA processing function of the nucleolus using light

Lian Zhu¹, Tiffany M. Richardson², Ludivine Wacheul³, Ming-Tzo Wei¹, Marina Feric¹, Gena Whitney¹, Denis L.J. Lafontaine³, and Clifford P. Brangwynne^{1,4*}

1. Department of Chemical and Biological Engineering, Princeton University
2. Department of Molecular Biology, Princeton University
3. RNA Molecular Biology, ULB Cancer Research Center (U-CRC), Center for Microscopy and Molecular Imaging (CMMI), Fonds de la Recherche Scientifique (F.R.S.-FNRS), Université Libre de Bruxelles (ULB), Belgium
4. Howard Hughes Medical Institute

Clifford P. Brangwynne
Email: cbrangwy@princeton.edu

This PDF file includes:

Supplementary text
Figs. S1 to S8
References for SI reference citations

Supplementary Information Text

Methods

Preparation of Mammalian and *X. laevis* Nucleoli

NPM1 (Sino Biological), FBL (Addgene), and RPA16 (Addgene) were cloned into the pHR-mCh, pHR-GFP, and pHR-Cry2olig plasmid. DNA fragments encoding the nucleolar proteins were inserted into the linearized pHR-mCh-Cry2WT (or Cry2olig) backbone using In-Fusion Cloning Kit (Takara). The resulting constructs were fully sequenced to confirm the absence of unwanted substitutions.

Mammalian NIH3T3 lentiviral cell lines expressing proteins (NPM1, FIB1, and RPA16) fused to mCherry (mCh)-Cry2olig and GFP were maintained at 37C using standard conditions. NPM1-mCh-CRY2olig CRISPR cell lines were generated in NIH3T3 cells through co-transfection of sgRNA-Cas9 plasmid and repair template followed by cell sorting to isolate a monoclonal cell line expressing NPM1-mCh-CRY2olig. sgRNA sequences were found using Target Finder (courtesy of Feng Zheng, crispr.mit.edu) and were cloned into the sgRNA-Cas9 plasmid (PX458, Addgene) following Zheng Lab cloning protocol. The repair template was constructed by using inserting a 750bp homology arm (with mutated PAM domain) starting at the C terminal end of the NPM1 gene followed by mCh-CRY2olig and a second 750bp homology arm into the PUC19 vector using In-Fusion (Takara) cloning. Cell line was verified by western blot and sequencing and maintained at standard conditions. FRAP measurements were also performed to verify CRY2olig response to 200nW 488nm light.

Frogs were anesthetized with 0.1% MS-222 solution, and oocytes were surgically removed from female *X. laevis* frogs following an IACUC approved protocol. Vector pCS2+ backbones were used for all fluorescent fusion constructs. mRNA of endogenous proteins (NPM1) with fluorescent (RFP, GFP, and Cerulean) and Cryolig tags were microinjected into oocytes as previously described [1]. Nuclei were manually dissected in mineral oil and subsequently imaged.

Fluorescence Correlation Spectroscopy

We used a laser scanning confocal microscope (Nikon A) and an oil immersion objective, (Plan Apo 60X/1.4, Nikon) combined with Fluorescence Correlation Spectroscopy (FCS) Upgrade Kit for Laser Scanning Microscopes (PicoQuant). FCS measurements were performed using the SymPhoTime Software (PicoQuant). Data for diffusion and concentration of proteins were obtained using 30s FCS measurement time. The measurements were performed on NIH3T3 cells expressing NPM1::mCh::Cry2olig, NPM1::mCh, and mCh::Cry2olig. For each measurement, the resulting auto-correlation functions were fitted applying the pure diffusion model below. Triplet state formation at short time scale (τ) was neglected due to low laser power used.

$$G(\tau) = G(0) \left(1 + \left(\frac{\tau}{\tau_D}\right)\right)^{-1} \left(1 + \left(\frac{\tau}{\kappa^2 \tau_D}\right)\right)^{-0.5}$$

Here, $G(0)$ is the magnitude at short timescales, τ is the lag time, τ_D is the half decay time, and κ is the ratio of axial to radial of measurement volume ($\kappa = \omega_z / \omega_{xy}$). $\omega_{xy} = 0.18$ mm and $\kappa = 5.1$ was calibrated using measurements of fluorophore dye Atto 550 in water. The parameters τ_D and $G(0)$ are optimized in the fit and are used to determine the diffusion coefficient ($D = \omega_{xy}^2 / 4\tau_D$) and molecule concentration

$(C = \left(\pi^{\frac{3}{2}} \omega_{xy}^2 \omega_z G(0) \right)^{-1})$ [2]. Here, the measurement volume is approximated by a

three-dimensional Gaussian with two parameters, ω_{xy} and ω_z . Mean and standard deviation of diffusion coefficient and concentration inferred from fitting correlation curves from 5-10 different cells. Beta is then calculated by taking the slope of the fitted lines of diffusion coefficient vs. concentration for each cell line.

Kinetic modeling of light activation

Cells were imaged on a laser scanning confocal (Nikon A1) at two separate laser powers (30nW and 90nW) with off interval times (T) of 15, 30, and 50s for 10-20mins. The nucleoplasmic intensity at the beginning and end of the imaging is extracted (subtracting the background intensity). The initial concentration (C_{tot}), final concentration ($C_{bg,st}$), blue light intensity, and T are used to determine k_1 and k_2 as per the model and methods in [29].

Actin disruption and coarsening in *X. laevis*

To disrupt actin, latrunculin A (Lat-A, Sigma) treatment was performed for 1-2 hours at 2 μ g/ml at constant rotation. After Lat-A treatment, nuclei were dissected in mineral oil and placed in an imaging chamber consisting of a glass coverslip and glass coverslide separated by a silicone well (Grace Biolabs) as previously described [3]. Movies capturing nucleoli consisted of 10-15 μ m z-stacks with 1-2 μ m step size and were acquired for several hours. Activated nucleoli were exposed to 100% 488nm laser light every 45s for exposure times of 100-200ms. Maximum intensity projections were made in each channel, and fusion events were analyzed at approximately 2 hours after the start of imaging.

Fluorescence Recovery After Photo-bleaching

NIH-3T3 cells expressing NPM1-mCh-Cry2olig, FBL-mCherry-Cry2olig, RPA16-mCherry-Cry2olig, NPM1-GFP, FIB1-GFP, and RPA16-GFP were photo-bleached with a spot ~ 1 μ m in diameter and the recovery of fluorescence intensity within the region of interest was obtained for each experiment. Intensity traces were normalized and the fraction recovery was taken at 300s. Cells were imaged using a heating stage at 37°C using a Nikon A1 laser scanning confocal using a 60X, 1.4 NA oil immersion objective.

Dextran experiments

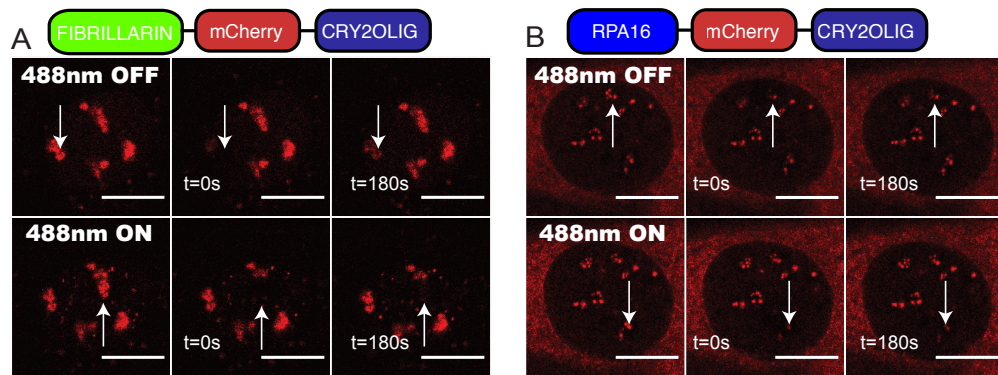
500k and 70k fluorescein isothiocyanate-dextran (Sigma) were directly injected into nuclei of *X. laevis* oocytes expressing NPM1::mCh::Cry2olig and NPM1::Cerulean. Nuclei were dissected in mineral oil 1-2 hours after microinjected and imaged using scanning confocal microscopy. FRAP was performed by photobleaching nucleoplasmic pockets in nucleoli

RNA analysis

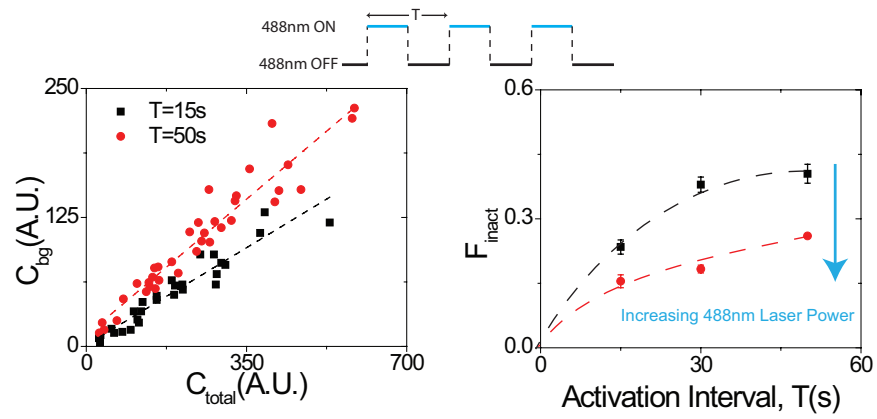
Cells were exposed to blue light (Teleopto LED array system, LED array model LEDA-X with driver LAD-1, setting 7.05) for 1-, 2-, or 3-days. Total RNA was extracted and northern blot were performed as in [4]. Experiment was done in 37C incubator.

The probes used are LD4100 5'-ACTGGTGAGGCAGCGGTCCGGGAGGCGC-3'; LD4096 5'-AGAGAAAAGAGCGGAGGTTCGGGACTCCAA-3'; LD4098 5'-ACAATGACCACTGCTAGCCTCTTCCCTT- 3'. Total RNA was separated on 2% agarose-formaldehyde denaturing gels. To achieve maximum resolution the RNAs were separated at 65 Volts for 22-hrs. Phosphor Imager quantification was performed with a Fuji FLA-7000 and the native software (Gauge). Normalization was performed by first dividing each rRNA species by their respective (CRY2 or untagged) raw intensity with no blue light exposure (t0 timepoint) and then by dividing the normalized value of NPM1-CRY2 by the control for each time-point. Three replicate northern blots were performed for each probe with the one shown representative of the three.

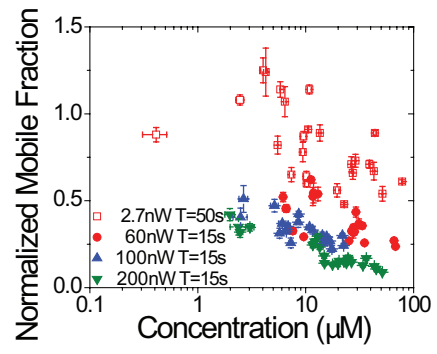
Supplemental Figures



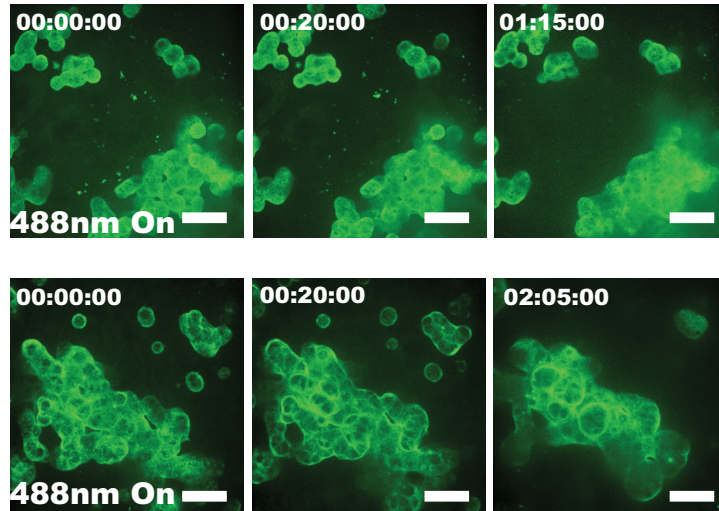
S1. Localization and FRAP images of Opto-Fibrillarlin and Opto-RPA16.



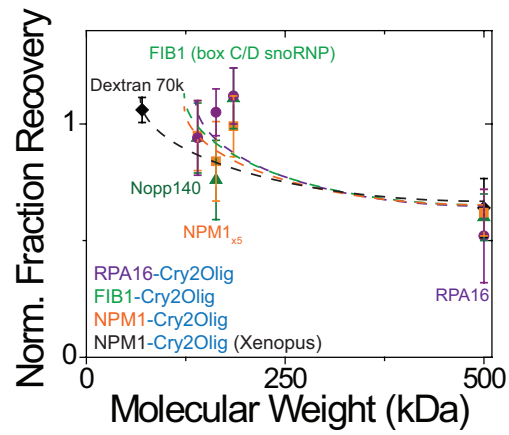
S2. Kinetic measurements of Opto-NPM1. (A) Concentration of nucleoplasmic background post activation vs. total concentration of nucleoplasm pre-activation. F_{inact} is proportional to the slope of this line, (B) F_{inact} plotted against the time between blue light or activation interval (T). These measurements were taken for two blue light intensities, 70nW (black) and 300nW (red).



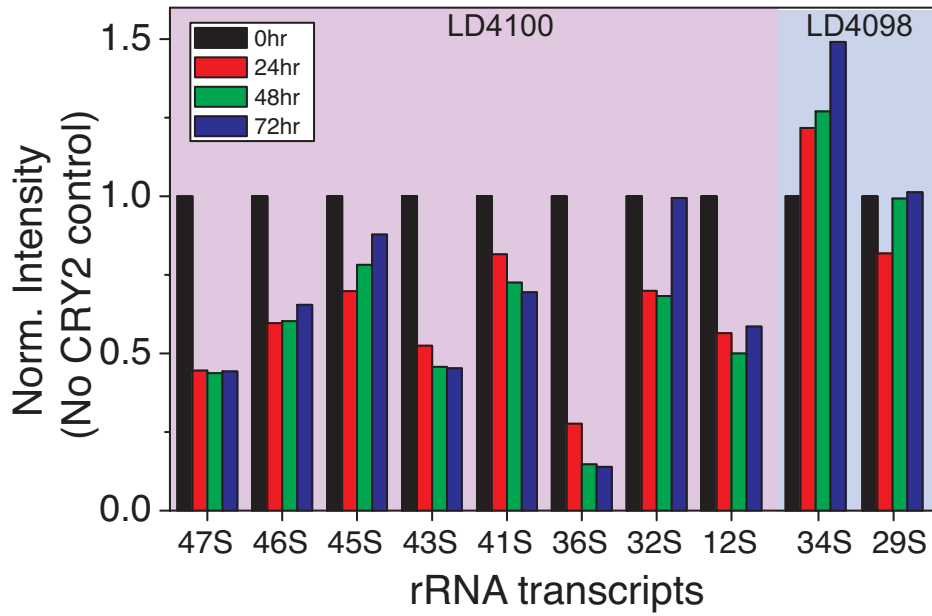
S3. Uncollapsed opto-NPM1 FRAP recovery at 300s vs. concentration of opto-NPM1 in the nucleolus.



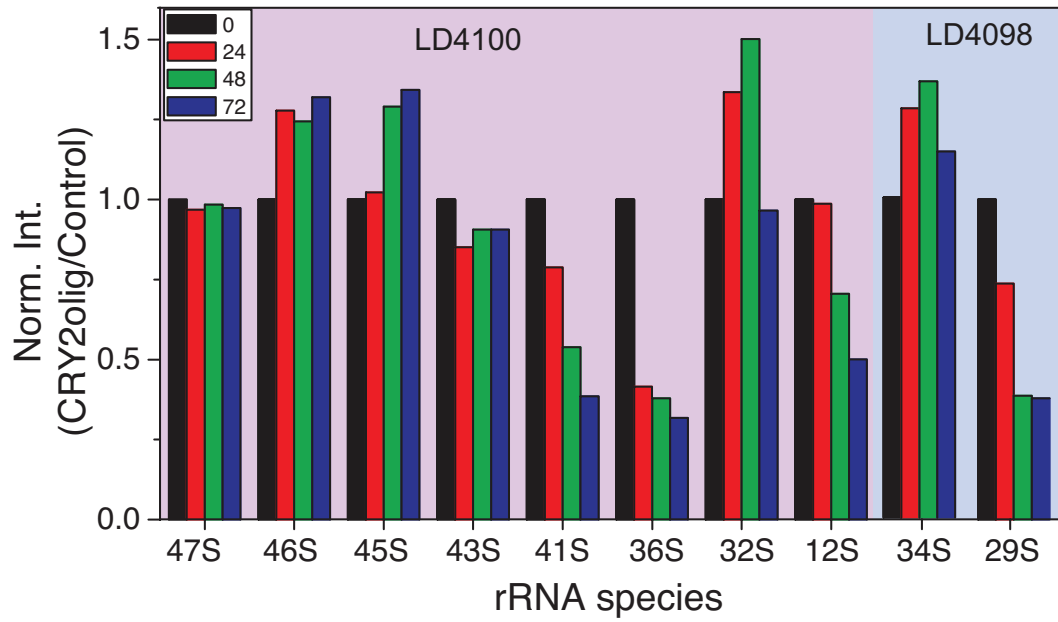
S4. Additional examples of activated opto-NPM1 in *Xenopus laevis*. In these, nucleoli already have begun fusing at start of imaging and blue light activation and despite nucleoli having fused initially, they do not fully relax over 2hrs.



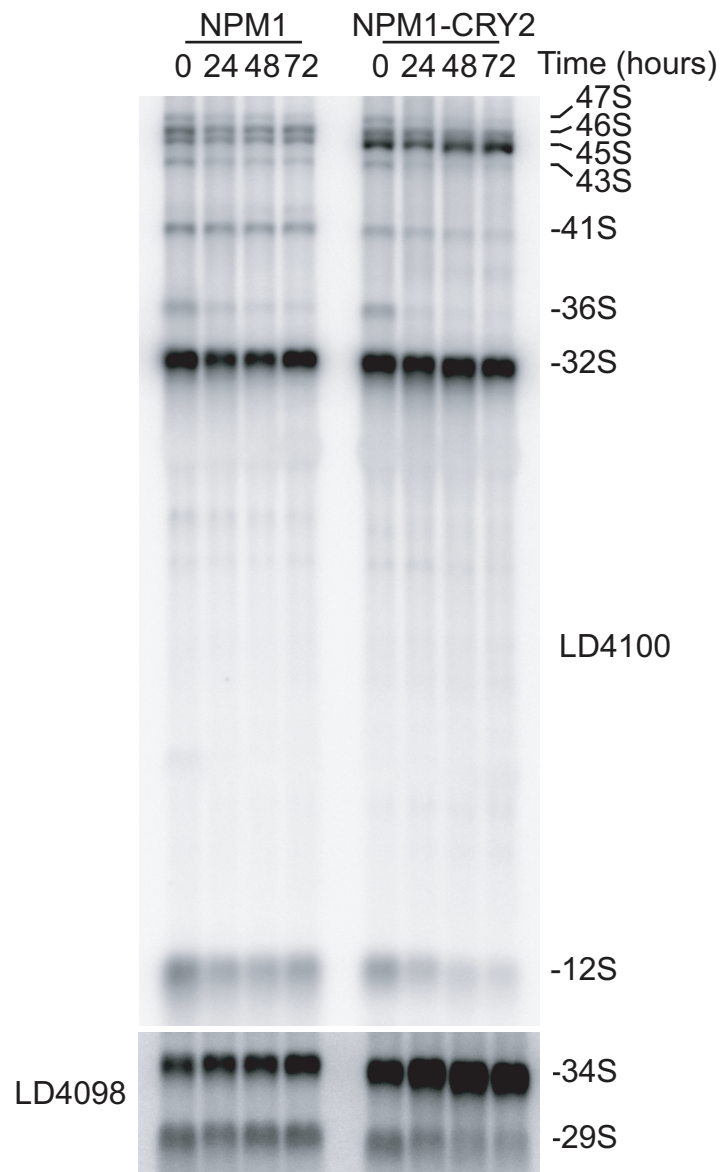
S5. Plot of FRAP recovery at 300s of GFP-tagged nucleolar proteins plotted by the molecular weight of the protein or the complex they are commonly found in when opto-nucleolar constructs are activated. Different colors represent the opto-nucleolar construct that is present and activated for each protein. Each data point is an average of 10-15 cells with error bars representing std. error of the mean.



S6. Northern blot quantification for NIH 3T3 (non-CRY2) control cells exposed to 0, 24, 48, and 72hrs of blue light. Data is normalized to T0 (0hrs of exposure to blue light) for each transcript.



S7. Northern blot quantification of all pre-rRNA species examined with the two probes. NPM1-CRY2 cells exposed to 0, 24, 48, and 72 hrs of blue light. Data is first normalized to T0 (0hrs of exposure to blue light) for each transcript and then divided by the normalized Control cells shown in S6.



S8. Northern blot of total RNA extracted from 3T3 cells expressing NPM1-CRY2, and from isogenic control cells exposed to blue light for indicated times. Northern blotting with probes LD4098, and LD4100 detects all major pre-rRNA precursors (see Fig. 6A for position of probes).

References

1. Feric M, Vaidya N, Harmon TS, Mitrea DM, Zhu L, Richardson TM, Kriwacki RW, Pappu RV, Brangwynne CP: **Coexisting Liquid Phases Underlie Nucleolar Subcompartments**. *Cell* 2016, **165**:1686-1697.
2. Krichevsky O, Bonnet G: **Fluorescence correlation spectroscopy: the technique and its applications**. *Reports on Progress in Physics* 2002, **65**:251-297.
3. Feric M, Brangwynne CP: **A nuclear F-actin scaffold stabilizes RNP droplets against gravity in large cells** *Nature Cell Biology* 2013, **15**.
4. Tafforeau L, Zorbas C, Langhendries JL, Mullineux ST, Stamatopoulou V, Mullier R, Wacheul L, Lafontaine DL: **The complexity of human ribosome biogenesis revealed by systematic nucleolar screening of Pre-rRNA processing factors**. *Mol Cell* 2013, **51**:539-551.